

Electronic Supplementary Information For:

**Highly Efficient Charge-Carrier Generation and Collection
in Polymer/Polymer Blend Solar Cells
with a Power Conversion Efficiency of 5.7%**

Daisuke Mori,^a Hiroaki Benten,^a Izumi Okada,^a Hideo Ohkita,^{a, b} and Shinzaburo Ito^a

^a*Department of Polymer Chemistry, Graduate School of Engineering, Kyoto University, Katsura, Nishikyo, Kyoto 615-8510, Japan, E-mail: benten@photo.polym.kyoto-u.ac.jp*

^b*Japan Science and Technology Agency (JST), PRESTO, 4-1-8 Honcho, Kawaguchi, Saitama 332-0012, Japan*

Experimental Details

Materials. The polymers PBDTTT-EF-T and N2200 were obtained from 1-Material Inc. and Polyera Corporation, respectively, and used as received. The weight-average molecular weight M_w , and polydispersity index (PDI; given by M_w/M_n , where M_n is the number-average molecular weight) of PBDTTT-EF-T as provided on the Certificate of Analysis were 115,000 g mol⁻¹ and 2.5, respectively. Those of N2200 were 178,000 g mol⁻¹ and 3.7, respectively. The M_w and PDI of N2200 were measured by size-exclusion chromatography (Shodex, GPC-101) using *o*-dichlorobenzene as the eluent, which was calibrated against monodisperse polystyrene standards (Shodex, STANDARD S-Series). The HOMO levels of the PBDTTT-EF-T and N2200 neat films were evaluated by photoelectron yield spectroscopy (Riken Keiki, AC-3). To evaluate their accurate HOMO levels, the bottom sides of their neat films were measured. Their LUMO levels were determined by adding the optical bandgap energy (E_g)

calculated from the 0-0 transition to the HOMO energy: E_g was calculated as 1.68 eV (PBDTTT-EF-T) and 1.55 eV (N2200) by using $E_g = hc/\lambda_{0-0}$, where h is the Planck's constant, c is the velocity of light, and λ_{0-0} is the wavelength of the crossing point between the absorption and PL bands of the neat films (Figure S6).

Device Fabrication and Measurements. ITO-coated glass substrates (10 Ω per square) were washed by ultrasonication with toluene, then acetone, and finally ethanol for 15 min each and then dried under an N_2 flow. The washed substrates were further treated with a UV- O_3 cleaner (Nippon Laser & Electronics Lab, NL-UV253S) for 30 min. A 40-nm-thick layer of PEDOT:PSS (H. C. Stark, PH-500) was spin-coated onto the ITO substrate at a spinning rate of 3000 rpm for 99 s and then dried in air at 140 $^\circ C$ for 10 min. A blended layer of PBDTTT-EF-T/N2200 was spin-coated onto the PEDOT:PSS film at 2500 rpm for 60 s from chlorobenzene solution. The blended solution was prepared by mixing PBDTTT-EF-T and N2200 in a 1:1 weight ratio in chlorobenzene: PBDTTT-EF-T (9 mg) and N2200 (9 mg) were dissolved in 1 mL of chlorobenzene. The thickness of the PBDTTT-EF-T/N2200 blended layers was 100 ± 10 nm. Preparation of the chlorobenzene solutions and subsequent spin coating of the solutions onto the PEDOT:PSS film was carried out in a N_2 -filled glove box. After the spin coating, the PBDTTT-EF-T/N2200 blended films were stored in a N_2 -filled glove box for one week at room temperature. Finally, a calcium interlayer (Ca, 2 nm) and an aluminum electrode (Al, 70 nm) were vacuum-deposited through a shadow mask at 2.5×10^{-4} Pa. The $J-V$ characteristics of the devices were measured using a direct-current voltage and current source/monitor (Advantest, R6243) under illumination by an "air mass 1.5-Global" (AM 1.5G) simulated solar light at 100 mW cm^{-2} . The light intensity was corrected with a calibrated silicon photodiode reference cell (Bunko-Keiki, BS-520; active area: 0.0534 cm^2). The spectral-mismatch factor calculated with respect to the AM 1.5G spectrum for the PBDTTT-EF-T/N2200 test-cell and BS-520 silicon reference-cell combination was 1.02.^{S1} The illumination intensity dependence of the $J-V$ characteristics was performed by using

reflective neutral density (ND) filters with optical densities (OD) from 0.1 to 1.5. The EQE spectrum was measured with a digital electrometer (Advantest, R8252) under illumination of monochromatic light from a 500-W Xe lamp (Thermo Oriel, model 66921) with optical cut filters and a monochromator (Thermo Oriel, UV–visible Cornerstone). The active area of the device was 0.07 cm², which was determined from the area of the top Ca/Al electrode. To minimize the *edge effect*, we used a device layout consisting of unpatterned PEDOT:PSS and PBDTTT-EF-T/N2200 layers sandwiched between unpatterned ITO and Ca/Al top electrodes. In this layout, the photoactive area can be assumed to be the area of the Ca/Al top electrode.^{S2} Simulated solar light was illuminated on the ITO side of the device. All measurements were carried out under an atmosphere of N₂ at room temperature. The device structure is depicted in Figure S7. More than 25 devices were fabricated to ensure the reproducibility of the *J–V* characteristics.

Mobility Measurements. Hole-only devices were fabricated by the following procedure. A PBDTTT-EF-T neat layer and PBDTTT-EF-T/N2200 blended layer were spin-coated onto separate ITO substrates covered with 40-nm-thick PEDOT:PSS, which acted as the anode. A gold electrode (Au, 50 nm) was then vacuum-deposited on each layer as the cathode (ITO|PEDOT:PSS|PBDTTT-EF-T|Au and ITO|PEDOT:PSS|PBDTTT-EF-T/N2200|Au). Thicknesses of the PBDTTT-EF-T neat layer and PBDTTT-EF-T/N2200 blended layer were 123 nm and 82 nm, respectively. Electron-only devices were fabricated by the following procedure. A 50-nm-thick Al layer, which acted as the anode, was vacuum-deposited on a glass substrate covered with 20-nm-thick poly(sodium 4-styrenesulfonate) ($M_w = 70,000$ g mol⁻¹). A neat layer of N2200 and PBDTTT-EF-T/N2200 blended layer were spin-coated onto each Al electrode. A Cs₂CO₃ interlayer (4 nm) and Al layer (80 nm) were then vacuum-deposited as the cathode (Al|N2200|Cs₂CO₃|Al and Al|PBDTTT-EF-T/N2200|Cs₂CO₃|Al). Thicknesses of the N2200 neat layer and PBDTTT-EF-T/N2200 blended layer were 145 nm and 95 nm, respectively. The Cs₂CO₃ layer was used to enhance the efficiency of electron

injection.^{S3} The dark $J-V$ characteristics of the devices were measured in air (hole-only devices) and under a N₂ atmosphere (electron-only devices) by using a direct-current voltage and current source/monitor (Advantest, R6243). The PBDTTT-EF-T and N2200 neat layers were spin-coated from chlorobenzene solutions. The PBDTTT-EF-T/N2200 blended layer was spin-coated under the same conditions used for device fabrication.

Photoluminescence Quenching Measurements. PL spectra were measured for the PBDTTT-EF-T and N2200 neat films and PBDTTT-EF-T/N2200 blended film, which were spin-coated onto quartz substrates, using a calibrated fluorescence spectrophotometer (Horiba, NanoLog). The sample films were excited at 500 nm to primarily excite the PBDTTT-EF-T component and at 400 nm to mainly excite the N2200 component. The excitation fraction of each component was 78% (PBDTTT-EF-T) and 72% (N2200). The PL quenching efficiency of PBDTTT-EF-T was evaluated from the ratio of PBDTTT-EF-T PL intensity for the PBDTTT-EF-T/N2200 blended films to that for a PBDTTT-EF-T neat film (after each PL intensity was corrected for variations in PBDTTT-EF-T absorption at 500 nm). The PL quenching efficiency of N2200 was evaluated from the ratio of N2200 PL intensity for the PBDTTT-EF-T/N2200 blended films to that for an N2200 neat film (after each PL intensity was corrected for variations in N2200 absorption at 400 nm).

Reflection Absorption Measurements. Absorbance was measured in reflection geometry at an incident angle of 5° normal to the substrate (Hitachi, U-4100) for the PBDTTT-EF-T/N2200 blended films covered with an Al top electrode. A schematic of the film structure used in reflection absorbance measurements is depicted in the inset of Figure S2. The blended film was spin-coated from chlorobenzene solution onto a glass substrate under the same conditions used for device fabrication. The reflection absorption of the PBDTTT-EF-T/N2200 blended films was calculated from the reflection absorbance ($Abs(\lambda)$) as $(1-10^{-Abs(\lambda)}) \times 100$.

AFM Measurements. Surface morphology of the PBDTTT-EF-T/N2200 blended film was observed by Atomic Force Microscopy (AFM, Simadzu, SPM-9600). Silicon probes were used with a resonant frequency of ~ 267 kHz and a force constant of ~ 42 N m $^{-1}$ (NANO WORLD, NCHR-10).

1. Device parameters

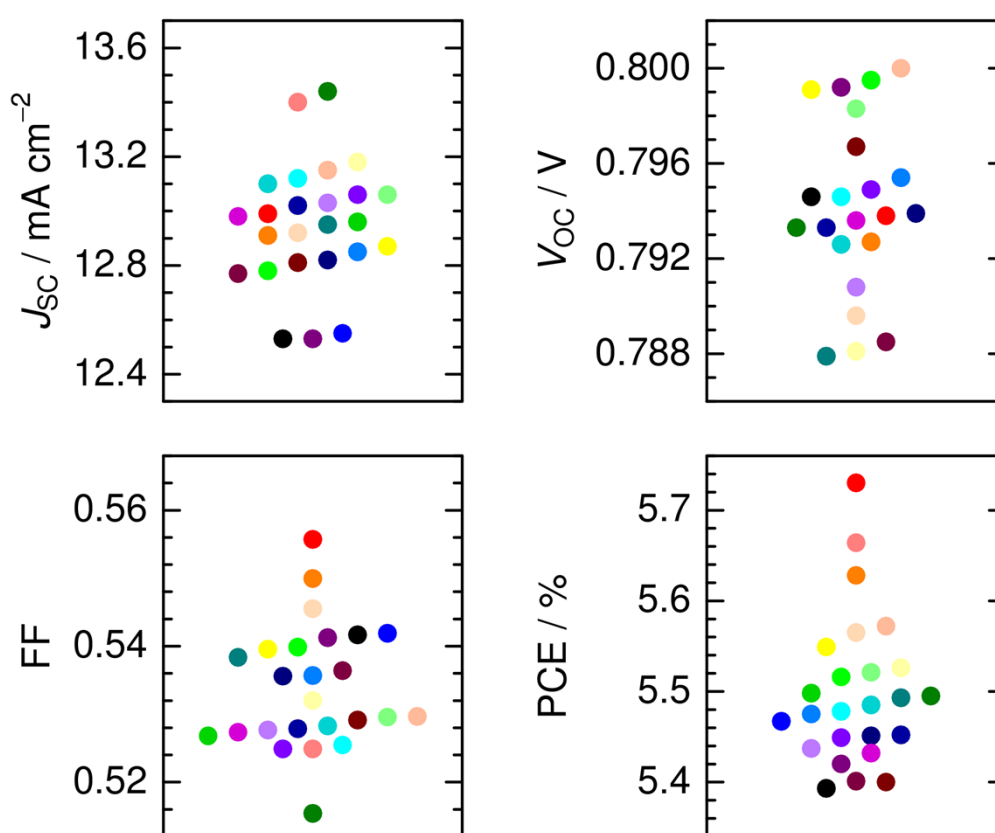


Fig. S1 Distributions of J_{sc} , FF, PCE, and V_{OC} of PBDTTT-EF-T/N2200 BHJ solar cells. Circles of the same color in each figure represent the parameters obtained from the same device.

2. Calculation of the number of photons absorbed by the PBDTTT-EF-T/N2200 layer

The number of photons absorbed by the PBDTTT-EF-T/N2200 blended film (N_{ph}) was calculated using the following equation:

$$N_{\text{ph}} = \int_{350\text{nm}}^{900\text{nm}} \frac{N_{\text{AM1.5G}}(\lambda) \cdot \%Abs(\lambda) \cdot d\lambda}{100} \quad (\text{S1})$$

In Equation S1, $N_{\text{AM1.5G}}$ is the number of photons from AM 1.5G solar light, %Abs is the percentage absorption of the PBDTTT-EF-T/N2200 blended film, and λ is the wavelength. The value of %Abs was calculated from the absorbance (Abs) of the blended film as $\%Abs(\lambda) = (1 - 10^{-\text{Abs}(\lambda)}) \times 100$. The absorbance was measured in reflection geometry at an incident angle of 5° normal to the substrate (Hitachi, U-4100) for the blended film covered with an Al top electrode. Figure S2 shows the reflection absorbance of the blended film used for the calculation of %Abs. The blended film was spin-coated from chlorobenzene solution onto a glass substrate under the same conditions used for device fabrication.

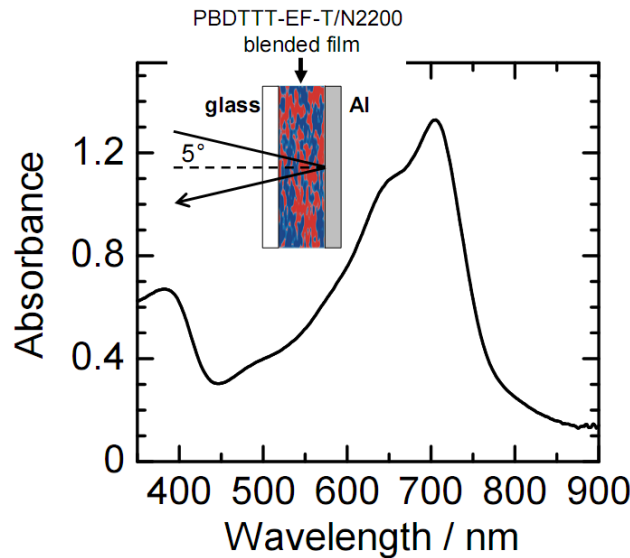


Fig. S2 Reflection absorbance spectrum of the PBDTTT-EF-T/N2200 blended film. The inset shows a schematic of the film structure used in the reflection absorbance measurement.

3. Mobility measurements

Charge-carrier mobilities (μ) were calculated from the dark J - V characteristics using the space-charge-limited current (SCLC) method using the Mott-Gurney equation for current

density J_{SCLC} , expressed as $J_{\text{SCLC}} = \frac{9}{8} \varepsilon_0 \varepsilon_r \mu \frac{V^2}{L^3}$, where ε_0 is the vacuum permittivity, ε_r is the

dielectric constant of the film ($\varepsilon_r = 3$ was assumed), and L is the thickness of the active

layer.^{S4, S5} The J - V characteristics of the hole-only devices and those of the electron-only

devices are shown in Figures S3-1 and S3-2, respectively.

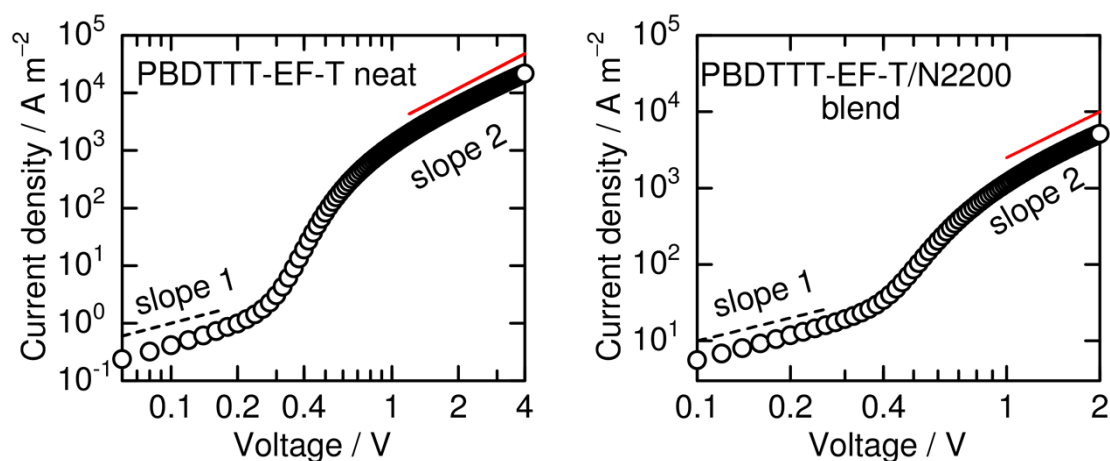


Fig. S3-1 The dark J - V characteristics of ITO|PEDOT:PSS|PBDTTT-EF-T(123 nm)|Au and ITO|PEDOT:PSS|PBDTTT-EF-T/N2200(82 nm)|Au hole-only devices.

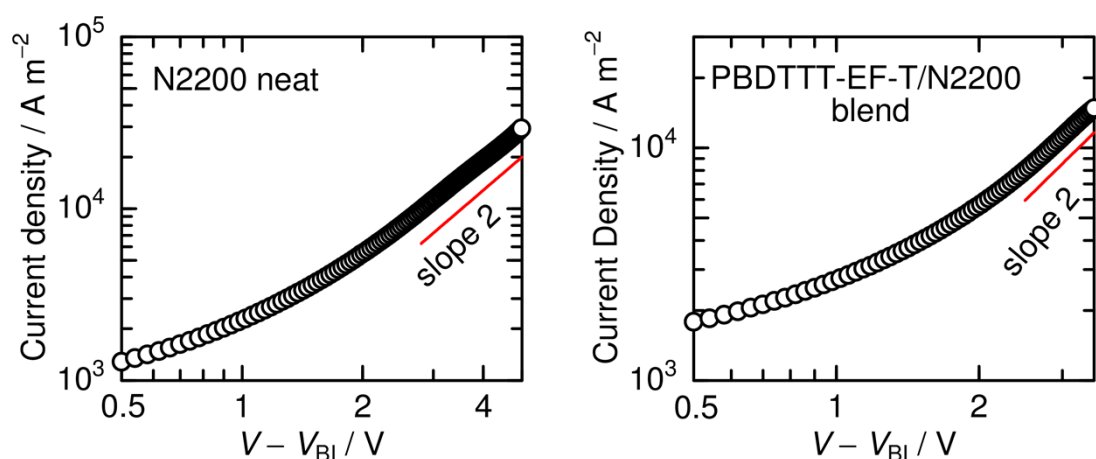


Fig. S3-2 The dark J - V characteristics of Al|N2200(145 nm)|Cs₂CO₃/Al and Al|PBDTTT-EF-T/N2200(95 nm)|Cs₂CO₃/Al electron-only devices. The applied voltage V was corrected for the built-in voltage V_{BI} of 2.1 V.^{S6, S7}

4. Dependence of charge-carrier mobilities on film thickness.

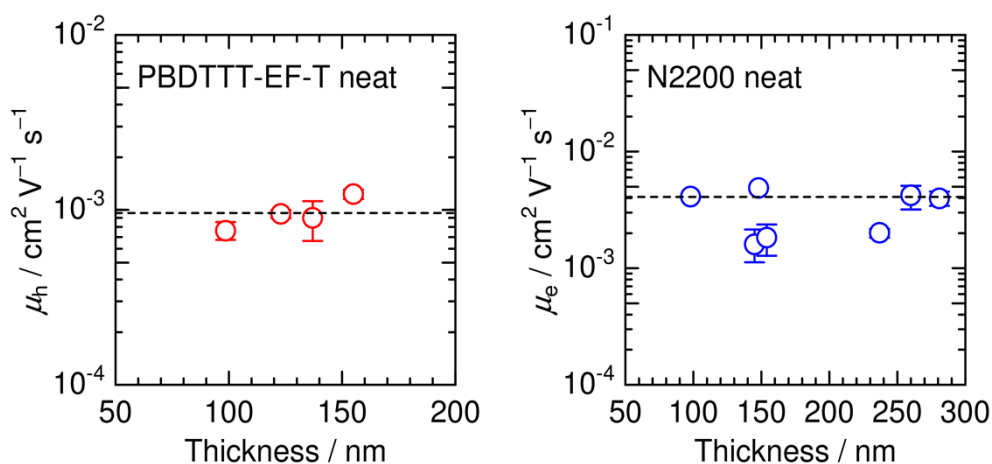


Fig. S4 Hole (μ_h) and electron (μ_e) mobilities of PBDTTT-EF-T and N2200 neat films evaluated for different film thickness.

Charge-carrier mobilities in the PBDTTT-EF-T/N2200 blended film calculated by considering the voltage drop due to contact resistance (the resistance of our cells was assumed to be 10Ω ^{S8, S9}) are $\mu_h = 4.1 \times 10^{-4} \text{ cm}^2 \text{V}^{-1} \text{s}^{-1}$ and $\mu_e = 4.8 \times 10^{-4} \text{ cm}^2 \text{V}^{-1} \text{s}^{-1}$, respectively

5. Dependence of FF on active layer thickness

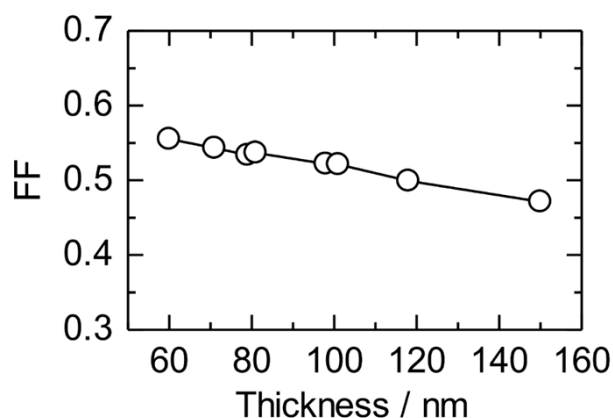


Fig. S5 FF of PBDTTT-EF-T/N2200 BHJ solar cells with varying thicknesses ranging from 60 nm to 150 nm under AM 1.5G illumination (100 mW cm^{-2}).

6. Calculation of optical bandgap energy (E_g)

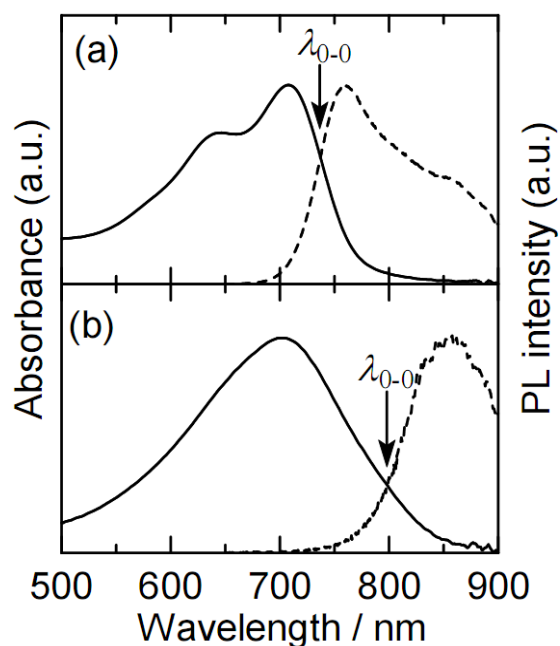


Fig. S6 Absorbance (solid line) and PL (dashed line) spectra of (a) PBDTTT-EF-T and (b) N2200 neat films spin-coated from chlorobenzene solution. The optical bandgap energy (E_g) was calculated from the 0-0 transition using $E_g = hc/\lambda_{0-0}$, where h is the Planck's constant, c is the velocity of light, and λ_{0-0} is the wavelength of the crossing point between the absorption and PL bands.

7. Device structure

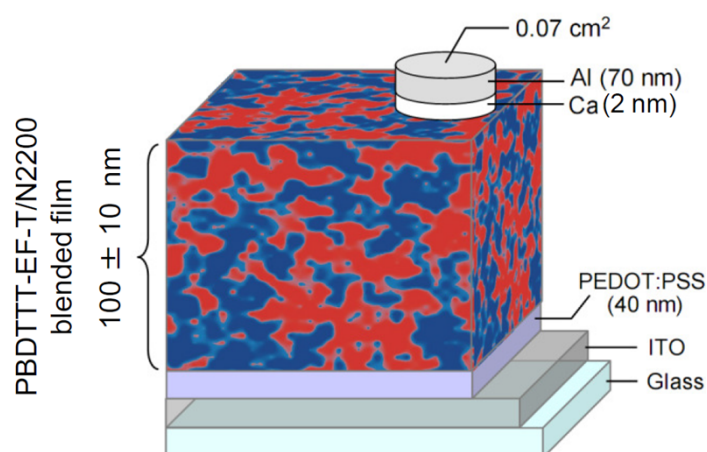


Fig. S7 Schematic illustration of the PBDTTT-EF-T/N2200 device structure.

References

- (S1) V. Shrotriya, G. Li, Y. Yao, T. Moriarty, K. Emery and Y. Yang, *Adv. Funct. Mater.* 2006, **16**, 2016.
- (S2) A. Cravino, P. Schilinsky and C. J. Brabec, *Adv. Funct. Mater.* 2007, **17**, 3906.
- (S3) G. J. A. H. Wetzelaer, M. Kuik, Y. Olivier, V. Lemaur, J. Cornil, S. Fabiano, M. A. Loi and P. W. M. Blom, *Phys. Rev. B* 2012, **86**, 165203.
- (S4) G. G. Malliaras, J. R. Salem, P. J. Brock and C. Scott, *Phys. Rev. B* 1998, **58**, R13411
- (S5) Y. Shen, A. R. Hosseini, M. H. Wong and G. G. Malliaras, *ChemPhysChem* 2004, **5**, 16.
- (S6) The V_{BI} was estimated from the difference in the work functions between the Al anode (4.3 eV) and $\text{Cs}_2\text{CO}_3/\text{Al}$ cathode (2.2 eV).^{S7}
- (S7) J. Huang, Z. Xu and Y. Yang, *Adv. Funct. Mater.* 2007, **17**, 1966.
- (S8) S. M. Tuladhar, D. Poplavskyy, S. A. Choulis, J. R. Durrant, D. D. C. Bradley and J. Nelson, *Adv. Funct. Mater.* 2005, **15**, 1171.
- (S9) Y. Liang, Z. Xu, J. Xia, S. T. Tsai, Y. Wu, G. Li, C. Ray and L. Yu, *Adv. Mater.* 2010, **22**, E135.